Original Article

Yuki Tokunaga and Takashi Watanabe*

An investigation of the factors controlling the chemical structures of lignin dehydrogenation polymers

https://doi.org/10.1515/hf-2022-0129
Received August 9, 2022; accepted November 8, 2022;
published online November 23, 2022

Abstract: Dehydrogenation polymer (DHP) is widely used as a model polymer of lignin. The chemical structure of DHP is highly affected by the synthesis conditions; however, the factors affecting DHP structure are not comprehensively understood. In this study, guaiacyl DHPs were synthesized to investigate the effects of reaction scale, pH, polymerization-enzyme activity, reaction media containing organic solvent, and differences between Zutropf (ZT) and Zulauf (ZL) modes on DHP properties. The DHPs were structurally characterized by size exclusion chromatography, ^{1}H-^{13}C HSQC NMR, and thioacidolysis with and without Raney nickel desulfuration. In ZT mode, smaller reaction scale significantly increased β-*O*-4 content, and β-*O*-4 formation was negatively correlated with the dose of polymerization-enzyme, horseradish peroxidase. Acidic condition (pH 4.0) in succinate buffer also increased the β-*O*-4 content of the DHP, although the α position of the DHP was acylated by the incorporation of succinic acid. DHPs prepared at pH 9.0 had high β-1 contents and low β-5 contents, while the reaction in 20% 1,4-dioxane markedly increased the molecular weight of the DHP. A systematic approach controlling the molecular structure of DHPs would increase their value as models for native and isolated lignins.

Keywords: dehydrogenation polymer; HSQC NMR; lignin; size exclusion chromatography; thioacidolysis.

***Corresponding author: Takashi Watanabe**, Research Institute for Sustainable Humanosphere (RISH), Kyoto University, Uji 611-0011, Japan, E-mail: twatanab@rish.kyoto-u.ac.jp
Yuki Tokunaga, Research Institute for Sustainable Humanosphere (RISH), Kyoto University, Uji 611-0011, Japan; and Graduate School of Bioresources, Mie University, Tsu 514-8507, Japan

1 Introduction

Lignin is the most abundant aromatic resource in nature and a potential alternative to petroleum-derived products (Ragauskas et al. 2014). Lignin is synthesized by radical coupling of coniferyl, sinapyl, and *p*-coumaryl alcohols, which comprise guaiacyl (G), syringyl (S), and *p*-hydroxyphenyl (H) nuclei, respectively (Boerjan et al. 2003). The chemical properties of lignin, such as G/S/H ratio and interunit linkages, are diverse and depending on species, location, and developmental state in plant tissues, as well as environmental stress (Campbell and Sederoff 1996). Furthermore, isolation of lignin by physical, chemical, or biological treatments alters their chemical structures (Ikeda et al. 2002; Liitia et al. 2003; Pu et al. 2015). Thus, lignin and its derivatives have highly heterogeneous structures, making the analysis and industrial application of lignin difficult. To understand the physico- and (bio) chemical behaviors of lignin, lignin model compounds such as monomer (Pan 2008), dimer (Hilgers et al. 2018; Sturgeon et al. 2014), and oligomer models (Tokunaga et al. 2021) have been used. Dehydrogenation polymer (DHP) is widely used as a lignin model polymer to investigate the chemical and biological reactivity of native lignin (Ando et al. 2013; Hofrichter et al. 1999; Johjima et al. 1999). In the preparation of DHP, monolignol is oxidized by laccase or peroxidase and spontaneously polymerized through radical coupling in aqueous buffers. The guaiacyl-type DHP contains several different types of interunit linkages, such as β-*O*-4, 5-5, 4-*O*-5, β-1, β-5, and β-β structures (Figure 1), and its HSQC NMR spectrum is similar to that of softwood lignin (Terashima et al. 2009). However, Sarkanen (1971) pointed out that the DHP has higher β-5 and β-β contents and lower β-*O*-4 content than softwood lignin, and the ratio of interunit linkages have been intensively investigated using thioacidolysis technique (Jacquet et al. 1997; Kishimoto et al. 2010). These differences in interunit linkage architecture decrease the validity of DHP usage as a model of native lignin.

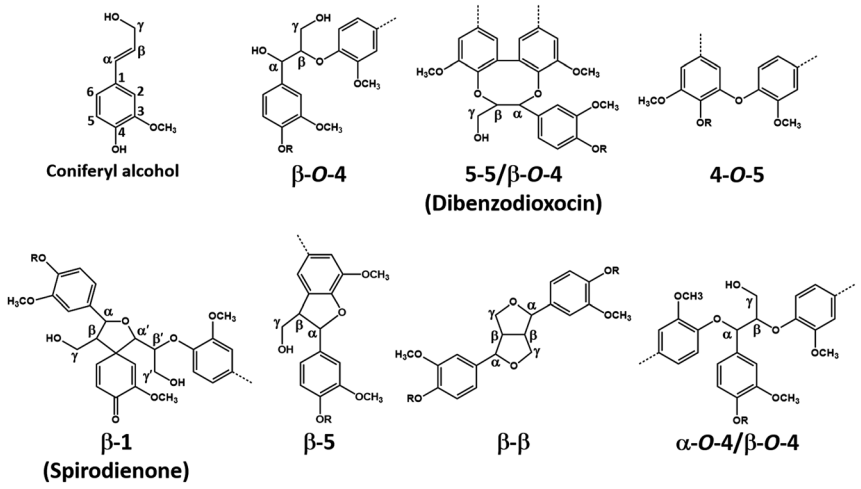

Figure 1: Chemical structures of a CA and the various interunit linkages in guaiacyl DHP. R indicates H or lignin.

To control the ratio of interunit linkages in DHP, extensive research effort has been dedicated to analyzing the factors affecting the DHP structures. When the monolignol is slowly and continuously added to a solution of oxidase, i.e., Zutropf (ZT) mode, DHP with higher β-*O*-4 content and molecular weight compared with DHP prepared by mixing monolignol and oxidase immediately in batch mode, i.e., Zulauf mode (ZL) (Cathala et al. 1998; Freudenberg 1956, 1968; Saake et al. 1996). Acidic conditions around pH 4.0 (Fournand et al. 2003; Grabber et al. 2003) and the presence of polysaccharides such as xylan (Barakat et al. 2007; Li et al. 2015), pectin (Terashima et al. 1996), and cyclodextrin (Nakamura et al. 2006) increase the β-*O*-4 contents of DHPs. The addition of organic solvents (Holmgren et al. 2008a; Hwang et al. 2015; Ikeda et al. 1998) and ascorbic acid (Holmgren et al. 2008b) also promote β-*O*-4 formation in DHP synthesis. In addition, fundamental parameters such as reaction scale, reaction time, and the amounts of monolignol, H_2O_2, and oxidase used greatly affect the chemical structure of the resultant DHPs. The structural variation of DHPs as determined by thioacidolysis is demonstrated in Table 1. All the DHPs reported in Table 1 were prepared in ZT mode using coniferyl alcohol (CA), H_2O_2, and horseradish peroxidase (HRP) at neutral pH. However, the weight-average molecular weights (*M*w) and β-*O*-4 contents of the resultant DHPs are diverse, probably due to differences in CA and H_2O_2 concentration, HRP activity, reaction time, pH, and temperature. Understanding the factors affecting the chemical structure of artificial lignin is essential for preparing DHPs that mimic native and isolated lignins.

In this study, 21 different DHPs were prepared from CA to assess the effects of reaction scale, pH, HRP activity, organic solvent, and the use of ZT or ZL mode on DHP structure. The structures of the DHPs were investigated by size exclusion chromatography (SEC), ^{1}H-^{13}C HSQC NMR, and thioacidolysis (with and without Raney nickel desulfuration). The relationships between the various synthetic parameters and the chemical structure of the DHP products are discussed in terms of the ratios of different interunit linkages, molecular weight, and amount of CA end group.

2 Materials and methods

CA and HRP were purchased from Wako Pure Chemical (Osaka, Japan). H_2O_2 was obtained from nacalai tesque (Kyoto Japan). Elemental analysis of DHPs was performed by the Laboratory for Organic Elemental Microanalysis in Kyoto University. Milled wood lignin (MWL) from Japanese cedar (*Cryptomeria japonica*) was prepared according to the method in our previous report (Tokunaga et al. 2019).

2.1 HRP activity assay

HRP activity was measured by the oxidation of guaiacol at 25 °C using a UV-2700 spectrophotometer (Shimadzu, Kyoto, Japan). The reaction mixture (3.1 mL) contained 0.32 mM guaiacol, 0.19 mM H_2O_2, and 0.04 μg of HRP in 100 mM sodium phosphate buffer (pH 6.5). The rate of guaiacol oxidation was calculated from the absorbance of cyclic tetraguaiacol (ε_{436nm} = 25.5 mM^{-1} cm^{-1}) at 436 nm (Tijssen 1985). For DHP synthesis in acidic (Table 2, entries 9, 10, and 14) and alkaline conditions (Table 2, entries 11, 12, and 15), 100 mM succinate buffer (pH 4.0) and 100 mM borate buffer (pH 9.0) were used instead of sodium phosphate buffer (pH 6.5). For DHP synthesis with an organic solvent (Table 2, entries 13–15), all the reaction mixtures contained 20% 1,4-dioxane. One unit of HRP was defined as the amount of enzyme that oxidases 1 μmol of guaiacol in 1 min at 25 °C under assay conditions.

Table 1: Synthetic conditions and molecular properties of previously reported DHPs.

References	Solution A	Solution B	Solution C	Stirring time[a]	Additional HRP	Product		
						*M*n	*M*w	Thioacidolysis monomer[b] (μmol/g)
Terashima et al. (1995, 1996)	CA (1.11 mmol) and HRP (4 mg) in PB [pH 6.5] (200 mL)	0.025% H_2O_2 (200 mL)	HRP (1 mg) in PB (2 mL)	67 h + 24 h (3 mL/h)	–	–	–	670
Cathala et al. (1998)	CA (1.66 mmol) in 1:9 (v/v) acetone/ 0.033 M PB [pH 6.1] (100 mL)	0.15% H_2O_2 (100 mL)	HRP (3 mg) in PB (300 mL)	20 h + 16 h (5 mL/h)	–	1410[c]	1830[c]	617[c]
Nakamura et al. (2006)	CA (0.56 mmol) in 0.1 M PB [pH 7.4] (10 mL)	0.5% H_2O_2 (4 mL)	HRP (2.2 mg) in PB (110 mL)	20 h + 6 h (0.2 or 0.5 mL/h)	–	2500	1600	590
Kishimoto et al. (2010)	CA (1.5 mmol) in 0.1 M PB [pH 6.5] (200 mL)	0.04% H_2O_2 (200 mL)	HRP (1 mg) in PB (50 mL)	48 h + 24 h (4.2 mL/h)	1 mg at 24 h	3180	10,440	488
Harman-Ware et al. (2017)	CA (0.55 mmol) in PPB [pH6.5] (100 mL)	0.04% H_2O_2 (95 mL)	HRP (1 mg) in 0.007% H_2O_2/ PPB (30 mL)	42 h + 30 h (2.4 mL/h)	1 mg at 24 h	1400	7700	404

All references synthesized DHPs from CA using ZT mode at neutral pH. In ZT mode, solutions A and B were slowly added to solution C to produce DHP. CA: coniferyl alcohol. HRP: horse radish peroxidase. PB: phosphate buffer. PPB: potassium phosphate buffer. [a]Stirring time with feeding of solutions A and B + stirring time after feeding of solutions A and B. The values in parentheses are the flow rates of solutions A and B. [b]Thioacidolysis monomer derived from β-*O*-4 structure. [c]Average values calculated from duplicate experiments.

Table 2: A summary of DHP synthetic conditions, yields, nitrogen contents, and molecular weights.

Entry	Method[a]	Volume of solution C[b] (mL)	pH	HRP activity (Unit)	Dioxane (%)	Product				
						Yield (%)	N (%)	*M*n	*M*w	*M*w/*M*n
1	ZT	300	6.5	100	0	40.7	0.0	1370	4282	3.13
2	ZT	300	6.5	313	0	40.8	0.1>	1320	5666	4.29
3	ZT	300	6.5	600	0	55.0	0.0	1119	3615	3.23
4	ZT	300	6.5	1500	0	62.0	0.1	988	3149	3.19
5	ZT	10	6.5	50	0	71.5	0.1>	1482	2985	2.01
6	ZT	10	6.5	150	0	74.3	0.1>	1289	2776	2.15
7	ZT	10	6.5	600	0	61.3	0.0	1336	2376	1.78
8	ZT	10	6.5	1500	0	82.6	0.2	1550	3402	2.19
9	ZT	300	4.0	145	0	56.2	0.1	1489	2467	1.66
10	ZT	300	4.0	290	0	66.7	0.3	1632	2550	1.56
11	ZT	300	9.0	150	0	37.1	0.1	1883	4233	2.25
12	ZT	300	9.0	300	0	46.7	0.1	2244	4497	2.00
13	ZT	300	6.5	150	20	38.7	0.1	1756	8028	4.57
14	ZT	300	4.0	150	20	39.2	0.3	2374	5509	2.32
15	ZT	300	9.0	150	20	22.2	0.5	2249	5459	2.43
16[c]	ZL	10	6.5	150	0	85.1	0.1>	1435	3042	2.12
17[c]	ZL	10	6.5	1500	0	87.4	0.1	1498	3731	2.49
18	ZL	300	6.5	150	0	76.9	0.0	1243	2773	2.23
19	ZL	300	6.5	1500	0	79.6	0.0	1383	2465	1.78
20	ZL	800	6.5	150	0	85.2	0.0	1283	2013	1.57
21	ZL	800	6.5	1500	0	86.4	0.0	1277	2207	1.73

[a]ZT and ZL modes were applied for DHP synthesis. [b]Solution C is 100 mM succinic acid, sodium phosphate, or boric acid buffer (pH 4.0, 6.5, or 9.0, respectively) containing 0 or 20% 1,4-dioxane and HRP with various activities. Solution A consists of the same buffer as solution C containing 1.5 mmol of CA and 3 mL of acetone. Solution B is 0.04% H_2O_2. [c]In entries 16 and 17, 70 and 20 mL of solutions A and B were added to the solution C, while other entries used 100 mL of solutions A and B.

2.2 Synthesis of DHPs in ZT mode (Table 2, entries 1–15)

Three solutions were prepared for DHP synthesis by the ZT mode at neutral pH (Table 2, entries 1–8). Solution A: 100 mM sodium phosphate buffer (100 mL, pH 6.5) containing 1.5 mmol CA and 3 mL acetone. Solution B: 0.04% H_2O_2 (100 mL). Solution C: 100 mM sodium phosphate buffer (300 or 10 mL, pH 6.5) containing HRP of various activities (50–1500 U). Solutions A and B were slowly added to the solution C with vigorous stirring over 24 h using a micro tube pump (MP-3, EYELA, Tokyo, Japan) at room temperature in the dark. After addition of solutions A and B, the mixture was stirred for an additional 20 h. The precipitate was collected by centrifugation (10,000 ×*g*, 10 min) and washed three times with distilled water before lyophilization. The obtained DHP was dissolved in 1,4-dioxane/water (9:1, *v/v*) and filtered through No. 131 qualitative filter paper (Advantec, Tokyo, Japan) for purification. The filtrate was lyophilized and dried *in vacuo* before analysis.

For DHP synthesis under acidic condition (Table 2, entries 9, 10, and 14), 100 mM succinate buffer (pH 4.0) was used instead of sodium phosphate buffer (pH 6.5). For DHP synthesis under alkaline condition (Table 2, entries 11, 12, and 15), 100 mM borate buffer (pH 9.0) was used instead of sodium phosphate buffer (pH 6.5). The synthesized DHP was recovered after the solution was acidified to pH 4.0 using 5 N HCl. For the procedures in Table 2, entries 13–15, solutions A and C contained 20% 1,4-dioxane.

2.3 Synthesis of DHPs in ZL mode (Table 2, entries 16–21)

Three solutions were prepared for DHP synthesis in ZL mode. Solution A: 100 mM sodium phosphate buffer (70 mL for the entries 16–17, and 100 mL for the entries 18–21, pH 6.5) containing 1.5 mmol CA and 3 mL acetone. Solution B: 0.04% H_2O_2 (20 mL for the entries 16–17, 100 mL for the entries 18–21). Solution C: 100 mM sodium phosphate buffer (10, 300, or 800 mL, pH 6.5) containing 150 or 1500 U HRP. Solutions A and B were simultaneously added to vigorously stirring solution C and the mixture was stirred for 44 h at room temperature in the dark. Procedures for the harvesting, washing, and purification of the DHPs were the same as those for ZT mode.

2.4 SEC

Each DHP (1 mg) was acetylated with pyridine (500 μL) and acetic anhydride (500 μL) at room temperature overnight. The molecular weight of the DHP acetates were determined by SEC using a Shimadzu liquid chromatography system equipped with an LC-20AD pump and an SPD M20A diode array detector (Shimadzu, Kyoto, Japan) at 40 °C. Three tandemly connected TSKgel SuperMultiporeHZ-M columns (Tosho, Tokyo, Japan) were used at 40 °C. The mobile phase was tetrahydrofuran (THF), and the flow rate was 0.35 mL/min. Polystyrene standard PStQuick C (Tosoh, Tokyo, Japan), vanillin, and 1-(3,4-dimethoxyphenyl)-2-(2-methoxyphenoxy)-1,3-propanediol were used for calibration.

2.5 NMR spectroscopy

DHPs (1.7–9.8 mg) were dissolved in DMSO-d_6 (Cambridge Isotope Laboratories, MA, USA) containing 200 μM 2,2-dimethyl-2-silapentane-5-sulfonic acid. All the 1D ^{1}H, 2D ^{1}H-^{13}C HSQC, and ^{1}H-^{13}C HMBC NMR spectra of the solutions (300 μL) were recorded using 5 mm Shigemi symmetrical microtubes (Shigemi, Tokyo, Japan) at 313 K on a Bruker Advance III 600 spectrometer equipped with a cryogenic probe and Z-gradient and controlled using Bruker Topspin-NMR software (ver. 3.5) (Bruker BioSpin, MA, USA). The signal for DMSO at δ_C/δ_H 39.5/2.49 ppm was used as an internal reference. NMR signals were assigned based on HMBC spectra and the literature (Gottlieb et al. 1997; Kim et al. 2008; Zeng et al. 2013).

2.6 Thioacidolysis and subsequent Raney nickel desulfuration

Thioacidolysis and subsequent Raney nickel desulfuration were performed according to previously described protocols (Lapierre et al. 1991; Roland et al. 1992). Monomer and dimer products were trimethylsilylated and quantified from their gas chromatography–mass spectrometry (GC–MS) total ion current chromatograms. Docosane was used as an internal standard, and its response factor of 0.5 was applied to quantify the main guaiacyl thioacidolysis monomer (Yue et al. 2012). Identification of mass peaks was performed based on previously reported mass fragmentation patterns (Kishimoto et al. 2010; Lapierre et al. 1991; Roland et al. 1992). GC–MS analysis was performed using a GCMS-QP 2010 SE system (Shimadzu, Kyoto, Japan) equipped with a DB-5MS column (30 m × 0.25 mm id, 0.25 μm film thickness: Agilent technologies, Santa Clara, CA, USA). The injection temperature was 250 °C, and trimethylsilylated samples (1 μL) were injected in split mode. Helium at a flow rate of 1.0 mL/min was used as the carrier gas. The column temperature program was set as 170 °C for 3 min, raised to 280 °C at 2 °C/min, and maintained for 20 min. Mass spectra were recorded in electron impact ionization mode at 70 eV.

2.7 Post-alkaline treatment of DHP

DHPs (15 mg, Table 2, entries 4, and 9) were dissolved in 1 mL of 1 M NaOH and incubated at 50 °C, 1000 rpm for 1 h using a Thermomixer Comfort (Eppendorf, Hamburg, Germany). The solutions were neutralized with 5 N HCl, and the precipitates were collected by centrifugation (10,000 ×*g*, 10 min) and washed three times with distilled water before lyophilization. These regenerated DHPs were analyzed by SEC, NMR, thioacidolysis, and Raney nickel desulfurization.

3 Results and discussion

3.1 Synthesis of DHPs

DHPs were prepared using the various conditions summarized in Table 2 to analyze the effects of reaction scale (10, 300, or 800 mL of solution C), pH (4.0, 6.5, or 9.0), HRP activity (50–1500 U), organic solvent (0 or 20% 1,4-dioxane), and synthetic mode (ZT or ZL) on the chemical structure of the resultant DHP.

The nitrogen contents of all the DHPs are less than 0.5%, indicating that the influence of remaining enzyme is

negligible. The yields of the DHPs are correlated with HRP activity except for Table 2, entry 7. Small-scale reactions (Table 2, entries 5–8) by the ZT mode gave higher DHP yields than the large-scale reactions (Table 2, entries 1–4). These results indicate that higher doses of HRP promote the polymerization of CA. ZL mode results in higher DHP yields compared with ZT mode when the same activity of HRP is used at the same reaction scale (compare Table 2, entries 4 and 19, 6 and 16, 8 and 17), suggesting that a high radical concentration is an important factor for DHP formation.

Addition of 20% 1,4-dioxane to the synthetic medium increases *M*w, although the DHP yields decrease (Table 2, entries 13–15). This increase in *M*w can be explained by the reactions of generating radicals to higher-molecular-weight polymeric fragments that are solubilized in the aqueous organic media, which allows exposure of the polymeric and oligomeric substrates to the radicals. The decrease in DHP yield is due to partial inactivation of the enzyme and decreased yield of the insoluble fraction after centrifugation of the reaction products. The DHPs obtained under alkaline conditions (Table 2, entries 11 and 12) also show higher *M*w with lower DHP yields because of the higher solubility of the phenolic polymers with ionized phenolic OH groups at high pH. Therefore, these results suggest that the solubility of DHP in solvents is an important factor affecting its molecular weight and the yield of water-insoluble fractions. This mechanism was supported by previous study reporting that usage of coniferyl alcohol γ-*O*-β-$_D$-glucopyranoside instead of coniferyl alcohol, increased molecular weight of the resultant DHP during polymerization due to its high water-solubility (Tobimatsu et al. 2006). We previously analyzed molecular conformation of β-*O*-4 lignin oligomer model using ^{1}H-^{1}H ROESY NMR and found that the lignin model has a more compact conformation in water compared with that in organic media (Tokunaga et al. 2021). Thus, the conformational change of DHP in organic media increases the sites accessible to radicals in the growing polymer with a concomitant increase in solubility of the polymer and reduced enzyme activity due to partial inactivation, resulting in the yields and polymerization degrees shown in Table 2, entries 13–15.

3.2 ^{1}H-^{13}C HSQC and HMBC NMR analyses of the DHPs

^{1}H-^{13}C HSQC spectra of aliphatic regions of the DHPs and Japanese cedar MWL are shown in Figure 2. In the HSQC spectrum of the entry-4 DHP (Figure 2A), HSQC signals from β-*O*-4, β-5, β-β, α-*O*-4, and 5-5/β-*O*-4 (dibenzo dioxocin) interunit linkages are clearly observed. Although the guaiacyl-type DHP and MWL present similar HSQC spectra (Figure 2A and F), the signals from α-*O*-4 to β-*O*-4 linkage are observed only in the DHP. α-*O*-4/β-*O*-4 bond is formed by nucleophilic addition of the phenolic hydroxy group of the lignin monomer or oligomer to the α position of the quinone methide structure possessing β-*O*-4 linkage. During lignin biosynthesis in plants, the supply rate of lignin monomers is assumed to be low, and nucleophilic addition of water and polysaccharides to quinone methide are preferentially occur than that of the lignin monomers. Thus, α-*O*-4/β-*O*-4 linkage is rarely observed in native lignin (Kilpeläinen et al. 1994) while this linkage is abundant in DHP (Terashima et al. 2009).

A comparison of Figure 2A–C provides insight into the effects of acidic and alkaline synthetic conditions on the interunit linkages in DHP. In the HSQC spectrum of DHP prepared under acidic pH (Figure 2B), α-*O*-4/β-*O*-4 signals are not observed, while signals for succinic acid, which was used as a buffer component, appear. This spectral change is explained by incorporation of succinic acid into the α position of the DHP through nucleophilic addition of the acid to quinomethide intermediates, resulting in the two new HSQC signals for α and β positions instead of α-*O*-4/β-*O*-4 signals. The proposed structure was confirmed by ^{1}H-^{13}C HMBC analysis (Figure 3A), which reveals a correlation between α_H and the carbonyl carbon of succinic acid. A proposed mechanism for the incorporation of succinic acid into DHP during polymerization is shown in Figure 3B.

In the HSQC spectrum of DHP synthesized under alkaline condition (Figure 2C), HSQC signals for the spirodienone (β-1) structure (Zeng et al. 2013; Zhang et al. 2006) are clearly observed. These signals are also observed for other DHP preparations and MWL, but their signal intensities are extremely low or below detectable levels, as shown in Figure 2. Thus, β-1 radical coupling that produces spirodienone structures is promoted in alkaline pH compared with neutral and acidic pH.

Figure 2D shows the HSQC spectrum of DHP prepared in the presence of 20% aq. 1,4-dioxane at neutral pH, and the spectrum is similar to that of DHP obtained without 1,4-dioxane (Figure 2A). This spectrum indicates that the presence of organic solvent has no effect on the variety of interunit linkages in DHP.

The HSQC spectrum of the DHP synthesized using ZL mode is shown in Figure 2E. The signal intensity for β-*O*-4 substructure with α-OH is quite low, while high-intensity signals for α-*O*-4/β-*O*-4 appear. These structural features are formed when the phenolic hydroxyl group of the lignin monomer, rather than water, is incorporated into quinone

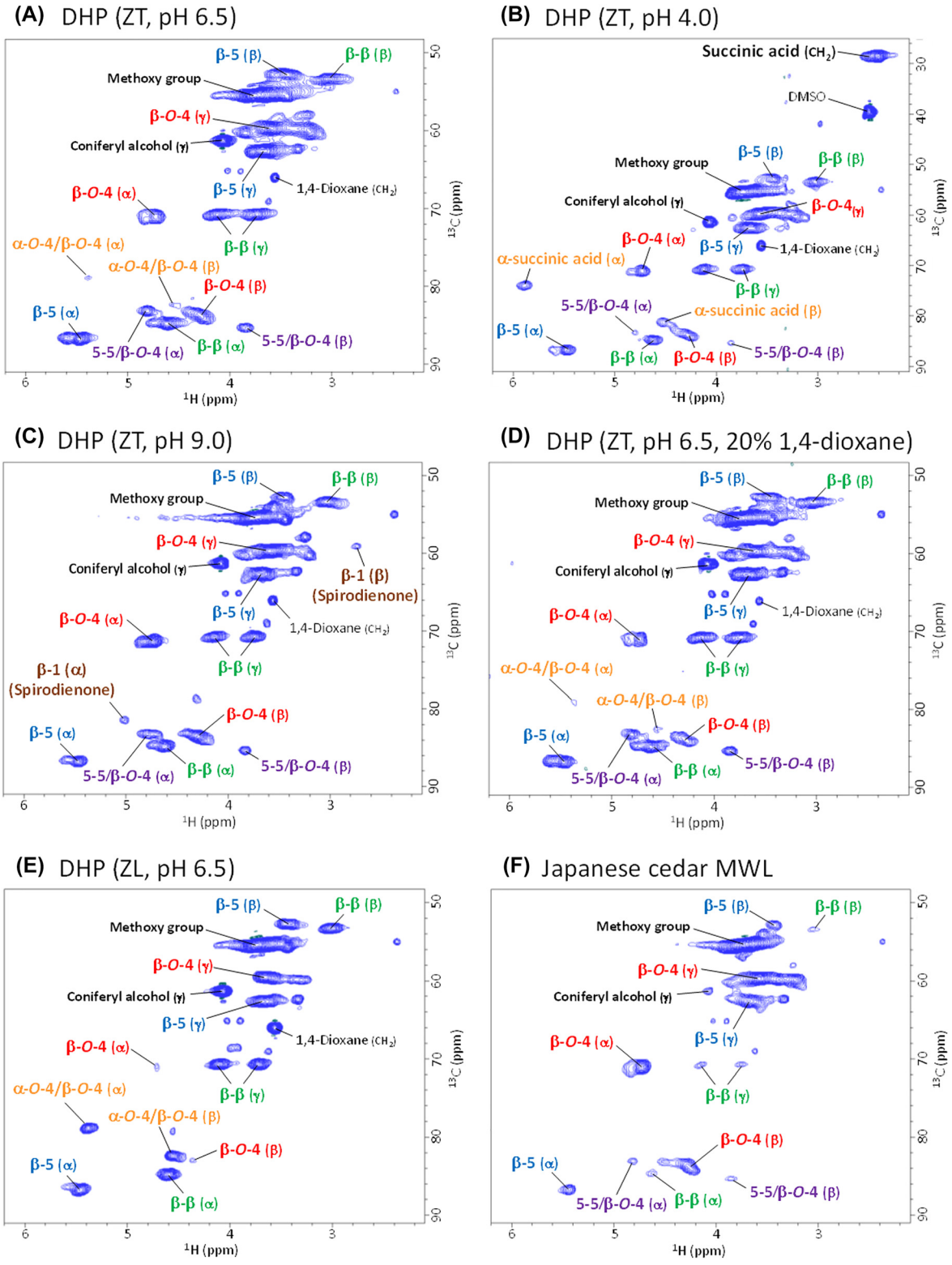

Figure 2: 2D ^{1}H-^{13}C HSQC spectra of aliphatic region of DHPs and Japanese cedar MWL. (A)–(E) HSQC spectra of DHPs from Table 2, entries 4 (2.2 mg), 9 (2.2 mg), 11 (2.1 mg), 13 (2.3 mg), and 16 (1.8 mg), respectively. (F) HSQC spectrum of Japanese cedar MWL (2.1 mg).

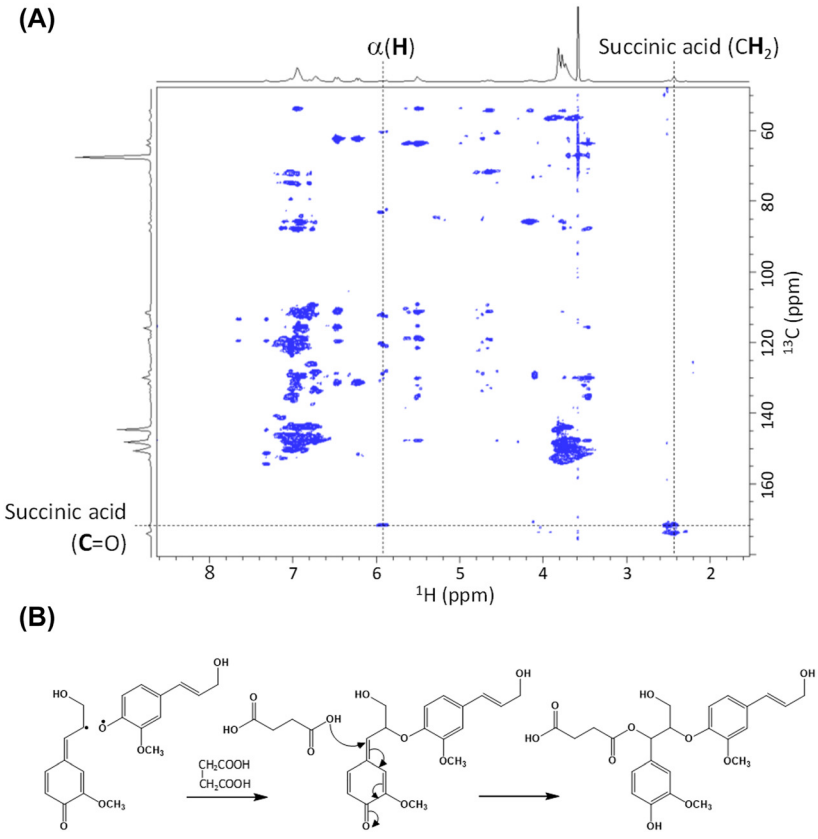

Figure 3: Incorporation of succinic acid into the α position of DHP during synthesis at pH 4.0. (A) HMBC spectrum of DHP prepared at pH 4.0 (Table 2, entry 10) indicating incorporation of succinic acid into the α position of DHP. (B) Reaction scheme illustrating the nucleophilic addition of succinic acid into a quinone methide intermediate during polymerization.

methide structures after β-*O*-4 formation because lignin monomer is highly abundant in the initial phase of ZL-mode synthesis.

3.3 Thioacidolysis and subsequent Raney nickel desulfuration

β-*O*-4 bond is the dominant interunit linkage in native lignin, but the presence of this bond in DHP is much lower than that in native lignin. Thus, increasing the β-*O*-4 content of DHP is required to prepare appropriate lignin models that possess structures similar to that of native lignin. The β-*O*-4 contents of the DHPs were evaluated by thioacidolysis, and the amount of thioacidolysis monomers derived from non-condensed β-*O*-4 and CA end groups are shown in Table 3.

All the DHPs have lower β-*O*-4 contents (218–426 μmol/g) than the Japanese cedar MWL (1039 μmol/g). For DHP synthesis in ZT mode, performing the reaction on a small scale significantly increases the β-*O*-4 content when the same HRP activity is used (Figure 4). A similar effect is partially observed for ZL mode (Table 3, entries 16–21). Factors affecting the chemical structure of DHP have been widely studied, but the importance of reaction scale on the β-*O*-4 content of DHP has not been addressed previously. When a small reaction scale is applied to DHP preparation, the monomer and oligomer concentrations are higher, which promotes aggregation of insoluble fractions and results in relatively high DHP yields (Table 2, entries 5–8). Several studies have demonstrated that the presence of the hydrophobic region of hemicellulose increases β-*O*-4 formation in lignin synthesis (Barakat et al. 2007; Tanahashi and Higuchi 1990). Similarly, the hydrophobic core provided by aggregated DHP may promote β-*O*-4 formation at a smaller reaction scale.

HRP activity is also an important factor affecting β-*O*-4 content. Mechin et al. (2007) reported that a low HRP dosage enhances the β-*O*-4 content of DHP. As shown in Figure 4, HRP activity is negatively correlated with the β-*O*-4 content in DHP. van Parijs et al. (2010) used a computer simulation of lignin biosynthesis to demonstrate that a decrease in the supply rate of monolignol increases β-*O*-4 formation with concomitant reduction of dimerization. This suggests that reactions with low-activity HRP increase β-*O*-4 content owing to the decreased influx rate of monolignol radicals during polymerization.

A remarkable increase in β-*O*-4 content is observed for acidic pH (Table 3, entries 9, 10, and 14). Moreover, combined use of pH 4.0 and low HRP activity (145 U)

Table 3: Monomer yields and relative percentages of dimeric products from thioacidolysis and subsequent Raney nickel desulfuration of DHP and MWL.

Entry[a]	Thioacidolysis		Raney nickel desulfurization					
	Main monomer (μmol/g)	CA end group (μmol/g)	5-5 (mol %)	4-*O*-5 (mol %)	β-1 (mol %)	β-5 (mol %)	β-β (mol %)	Total dimer yield (μmol/g)
1	284	58	29	2	10	51	9	61
2	265	57	35	1	18	41	4	31
3	263	58	24	1	9	51	15	51
4	222	64	28	1	20	49	2	36
5	396	84	15	1	8	61	16	134
6	364	97	17	1	7	60	15	129
7	368	82	13	1	6	65	16	139
8	276	72	24	2	6	58	10	89
9	426	82	34	2	14	42	8	48
10	345	66	41	2	17	36	4	30
11	306	112	43	1	34	18	4	49
12	238	92	34	1	52	11	2	22
13	293	88	21	1	19	48	11	18
14	386	59	24	1	21	44	11	13
15	319	46	22	1	43	26	8	15
16	283	248	3	0	1	59	37	92
17	314	171	5	1	2	58	34	69
18	218	190	3	0	1	56	40	63
19	239	143	5	1	2	56	36	62
20	225	173	2	0	1	57	38	74
21	237	127	4	1	2	65	28	50
Japanese cedar MWL	1039	42	24	1	66	8	0	35

[a]Entries are the same as those described in Table 2.

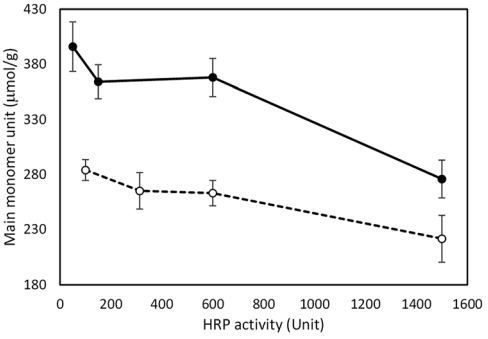

Figure 4: Effects of HRP activity and reaction scale on the β-*O*-4 content of DHPs synthesized in ZT mode. (○) DHP prepared using 300 mL of solution C (Table 2, entries 1–4), (●) DHP prepared using 10 mL of solution C (Table 2, entries 5–8). Experiments were performed three times, and the results are expressed as average values.

produces the most thioacidolysis monomer (Table 3, entry 9, 426 μmol/g) originating from β-*O*-4 bond. Grabber et al. (2003) reported that synthesis at pH 4.0 increases β-*O*-4 content compared with that at pH 5.5 in end-wise polymerization. In contrast, the β-*O*-4 contents of DHPs synthesized under alkaline pH (Table 3, entry 11: 306 μmol/g, and entry 12: 238 μmol/g of the thioacidolysis monomer) are similar to those of DHPs prepared under neutral pH (Table 3, entries 1 and 2, 284 and 265 μmol/g, respectively). The addition of 20% 1,4-dioxane (Table 3, entry 13) also has no apparent effect on the amount of thioacidolysis monomer (293 μmol/g). No synergistic effect of organic solvent and pH is observed when 1,4-dioxane is used in acidic or alkaline pH (Table 3, entries 14 and 15).

The abundance of 5-5, 4-*O*-5, β-1, β-5, and β-β interunit linkages (Figure 1) adjacent to β-*O*-4 bond were determined by Raney nickel desulfuration after thioacidolysis. As shown in Table 3, entries 1–8, DHPs prepared in ZT mode at neutral pH have lower β-1 contents and higher β-5 and β-β contents than those of Japanese cedar MWL. DHPs prepared in ZL mode (Table 3, entries 16–21) show extremely low 5-5 and β-1 contents and high β-β contents. β-β linkages are produced by monomer-monomer coupling, whereas 5-5 linkages are obtained by oligomer-oligomer coupling (Ralph et al. 2004). For DHP synthesis in ZL mode, high monomer radical concentrations induce more monomer-monomer coupling than oligomer-oligomer coupling,

resulting in abundant β-β and decreased 5-5 bond formation during DHP synthesis. Almost all 5-5 linkage form dibenzodioxocin structure (Rinaldi et al. 2016), and this structure is not indicated by the HSQC spectrum of DHP prepared in ZL mode (Figure 2E). Thus, the HSQC spectrum supports the result from Raney nickel desulfuration experiments after thioacidolysis. Acidic pH (Table 3, entries 9 and 10) slightly increases the 5-5 content and decreases the β-5 content compared with neutral pH. Interestingly, alkaline pH (Table 3, entries 11 and 12) significantly increases the β-1 content and decreases the β-5 content, and the DHP for Table 3, entry 12 has similar molar percentages of 5-5, 4-*O*-5, β-1, β-5, and β-β linkages to those of Japanese cedar MWL. The abundance of β-1 structures in the DHPs prepared at pH 9.0 is confirmed by its HSQC spectrum, which presents signals from spirodienone substructure (Figure 2C). The use of 1,4-dioxane in DHP synthesis (Table 3, entry 13) has no significant effect on the interunit linkages of the DHP, as also indicated by HSQC analysis (Figure 2D).

Comparison of the DHP products having similar molecular weight distributions, the amount of CA end groups reflects the frequency of structure branching in the DHP. 4-*O*-5 and 5-5/β-*O*-4 (dibenzodioxocin) linkages are branching points in native lignin. Furthermore, unlike native MWL, DHP has α-*O*-4/β-*O*-4 structure as the other branching point. ZL mode significantly increases the CA end group content (127–248 μmol/g) compared with ZT mode (57–97 μmol/g) at pH 6.5, which is explained by abundant α-*O*-4/β-*O*-4 structures in the DHPs synthesized using ZL mode (Figure 2E). Small-scale preparation also increases CA end group content. In ZT mode, small-scale reactions give slightly higher amounts of CA end groups (Table 3, entries 5–8, 72–97 μmol/g) compared with large-scale reactions (Table 3, entries 1–4, 57–64 μmol/g). For ZL mode, the amounts of CA end groups decrease in the order entry 16 (248 μmol/g) > entry 18 (190 μmol/g) > entry 20 (173 μmol/g), which were prepared using 10, 300, and 800 mL of solution C, respectively. The higher contents of CA end groups for smaller reaction systems are possibly related to the frequency of α-*O*-4/β-*O*-4 linkages preferentially formed in small-scale reactions.

3.4 Post-alkaline treatment of DHPs

Incorporation of succinic acid into the α position of DHP synthesized under acidic pH is demonstrated in the HSQC and HMBC spectra (Figures 2B and 3A). Because the incorporated succinic acid may have non-negligible effects on the DHP properties and unintentionally decrease its value as a lignin model polymer, the acyl groups were removed by saponification. The DHP prepared under acidic pH (Table 2, entry 9) was dissolved in 1 N NaOH, incubated at 50 °C for 1 h, and precipitated by neutralization. The precipitate was collected by centrifugation, washed three times with water, and lyophilized before analysis. For comparison, a DHP prepared under neutral pH (Table 2, entry 4) was also used in this experiment. The DHPs prepared by post-alkaline treatment are termed 'regenerated DHPs'.

Figure 5 shows a HSQC spectrum of aliphatic region of a regenerated DHP originally prepared under acidic pH. Comparison of the HSQC spectra obtained before and after alkaline treatment (Figures 2B and 5, respectively) show that the HSQC signals for succinic acid and the α position of DHP acylated with succinic acid disappear upon alkaline treatment. The HSQC signals for other interunit linkages show no significant changes, confirming that no side reactions such as degradation and condensation occur during alkaline treatment. The results of SEC, thioacidolysis, and Raney nickel desulfurization are summarized in Table 4. The yields of the regenerated DHPs are around 70%. This recovery loss may cause increases in molecular weight and β-*O*-4 content. The β-*O*-4 content of the DHP originally prepared at pH 4.0 (Table 2, entry 9) increases from 426 to 535 μmol/g upon alkaline treatment. This is the highest β-*O*-4 content of all the synthesized DHPs. In contrast, the regenerated DHP originally prepared at neutral pH shows only a slight increase in β-*O*-4 content. Thus, alkaline treatment effectively removes succinic acid incorporated into the α position of DHP without unwanted side reactions.

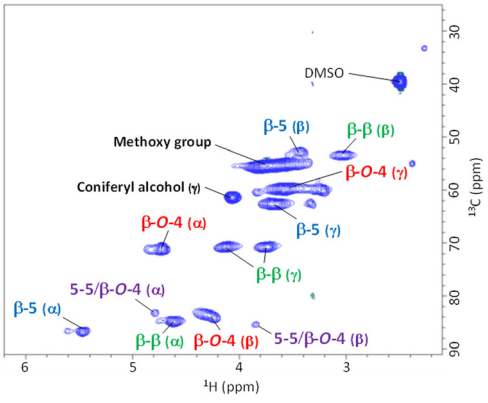

Figure 5: A 2D ^{1}H-^{13}C HSQC spectrum of aliphatic region of regenerated DHP derived from the Table 2, entry 9 product (1.7 mg). DHP from Table 2, entry 9 was dissolved in 1 N NaOH and subsequently precipitated by neutralization to prepare the regenerated DHP.

Table 4: Summary of SEC analysis, thioacidolysis, and Raney nickel desulfurization results for regenerated DHPs.

Sample[a]	Yield[b] (%)	Molecular weight			Thioacidolysis		Raney nickel desulfurization					
		Mn	*Mw*	*Mw*/*Mn*	Main monomer (μmol/g)	CA end group (μmol/g)	5-5 (mol %)	4-*O*-5 (mol %)	β-1 (mol %)	β-5 (mol %)	β-β (mol %)	Total dimer yield (μmol/mg)
Regenerated DHP from entry 4 (ZT, pH 6.5, 1500 U of HRP)	69.1	2178	7009	3.22	285	65	26	2	6	55	12	75
Regenerated DHP from entry 9 (ZT, pH 4.0, 145 U of HRP)	73.9	2609	5295	2.03	535	135	29	2	7	49	14	84

In the alkaline regeneration process, original DHPs (entries 4 and 9) were dissolved in 1 N NaOH and subsequently precipitated by neutralization to obtain regenerated DHPs. [a]Entries are the same as those described in Table 2. [b]Yields calculated based on weight of DHPs before and after alkaline regeneration.

3.5 Effects of synthesis conditions on DHP properties

The effects of reaction scale, pH, HRP activity, organic solvent, and the use of ZT or ZL mode on DHP synthesis are illustrated by the heat map in Figure 6 using entry 1 DHP as a standard for comparison. Synthesis in ZT mode with a small reaction scale (Table 2, entry 5) and ZL mode (Table 2, entry 18) show increased DHP yields and CA end group contents. For DHP synthesis under these conditions, the molecular weights are lower, and the β-β content is increased while 5-5 and β-1 contents are decreased. Compared to the entry 1 DHP, higher β-*O*-4 contents are obtained by small-scale ZT-mode reactions but lower β-*O*-4 contents are observed for ZL mode. Acidic pH (Table 2, entry 9) increases the β-*O*-4 and CA end group contents, and the highest β-*O*-4 content is obtained for the entry 9 DHP after post-alkaline treatment. Alkaline pH (Table 2, entry 11) increases the amount of CA end group and highly affects the distribution of interunit linkages, with increased β-1 and 5-5 ratios as well as decreasing in β-5 and β-β ratios. Addition of 1,4-dioxane to the aqueous medium (Table 2, entry 13) increases the molecular weight of the resultant DHP. Thus, the chemical structures of DHPs can be systematically controlled by employing different synthesis conditions, as shown in Figure 6.

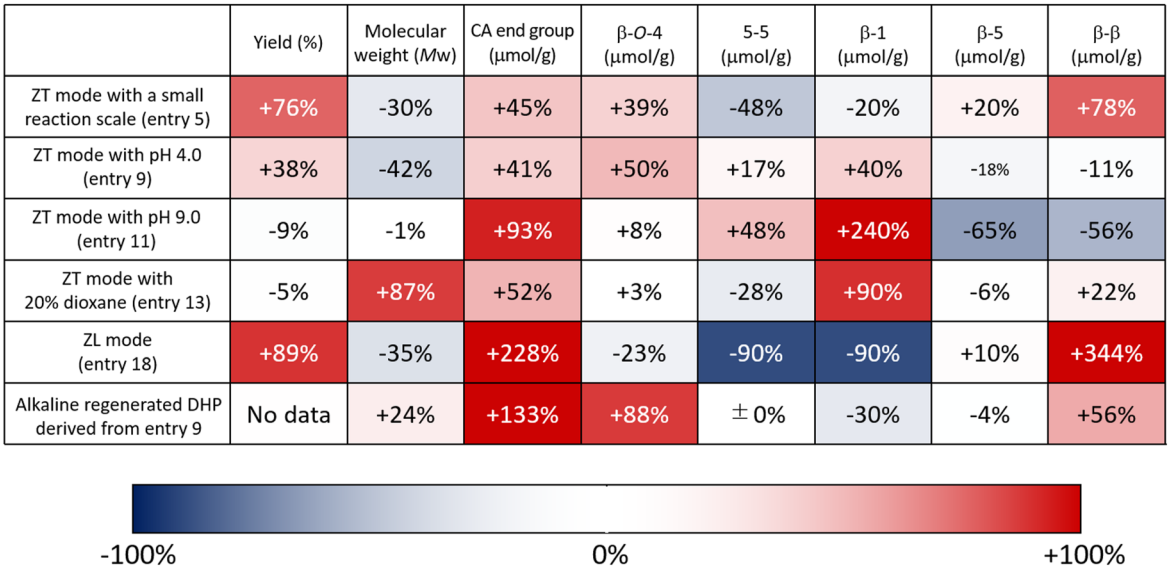

Figure 6: Heat map visualization of the effects of various synthesis conditions on DHP structure. Relative percentages were calculated in comparison with the product of the conditions from Table 2, entry 1, which was prepared using ZT mode with 300 mL of solution C (pH 6.5) containing 100 U HRP. Increases and decreases in the structural parameters are visualized by red and blue gradations, respectively. Significantly increased values higher than 100% are color-coded as red.

4 Conclusions

DHP is widely used as a synthetic polymer model of lignin. However, differences between the chemical structure of DHP and native lignin limit its validity as a lignin model. For instance, guaiacyl DHP has higher β-5 and β-β contents and lower β-*O*-4 and β-1 contents than softwood native lignin. To prepare DHP with structures similar to native lignin and isolated lignin, control of chemical structures of DHP is required. However, understanding the relationship between DHP structure and its synthesis conditions remains limited.

In the present study, 21 guaiacyl DHPs were prepared to investigate the structural effects of different synthesis conditions, such as molecular weight, amount of CA end group, β-*O*-4 content, and ratio of other interunit linkages in DHP.

The β-*O*-4 content of DHP is negatively correlated with reaction scale and HRP activity. DHP prepared under acidic pH has a high β-*O*-4 content, and post-alkaline treatment provided DHP with the highest β-*O*-4 content. Alkaline pH facilitates β-1 and 5-5 formation and suppresses β-5 and β-β formation during DHP synthesis. The presence of 1,4-dioxane increases the molecular weight of the DHP.

Thus, factors controlling the chemical structure of DHPs have been systematically analyzed in detail. In particular, the effects of reaction scale on DHP structure are clearly pointed out. This systematic approach correlates the various reaction conditions with DHP structure, thereby increasing the value of DHPs as models for native and isolated lignins.

Author contributions: All the authors have accepted responsibility for the entire content of this submitted manuscript and approved submission.

Research funding: This work was supported by JSPS KAKENHI grant number JP18J20331, Mission 2 research of RISH, and joint usage/research programs of IAE (ZE2021A-10).

Conflict of interest statement: The authors declare that they have no conflicts of interest regarding this article.

References

Ando, D., Nakatsubo, F., Takano, T., Nishimura, H., Katahira, M., and Yano, H. (2013). Multistep degradation method for β-O-4 linkage in lignins: γ-TTSA method. Part 2: reaction of lignin model polymer (DHP). Holzforschung 67: 249–256.

Barakat, A., Chabbert, B., and Cathala, B. (2007). Effect of reaction media concentration on the solubility and the chemical structure of lignin model compounds. Phytochemistry 68: 2118–2125.

Boerjan, W., Ralph, J., and Baucher, M. (2003). Lignin biosynthesis. Annu. Rev. Plant Biol. 54: 519–546.

Campbell, M.M. and Sederoff, R.R. (1996). Variation in lignin content and composition. Mechanisms of control and implications for the genetic improvement of plants. Plant Physiol. 110: 3–13.

Cathala, B., Saake, B., Faix, O., and Monties, B. (1998). Evaluation of the reproducibility of the synthesis of dehydrogenation polymer models of lignin. Polym. Degrad. Stabil. 59: 65–69.

Fournand, D., Cathala, B., and Lapierre, C. (2003). Initial steps of the peroxidase-catalyzed polymerization of coniferyl alcohol and/or sinapyl aldehyde: capillary zone electrophoresis study of pH effect. Phytochemistry 62: 139–146.

Freudenberg, K. (1956). Beiträge zur Erforschung des Lignins. Angew. Chem. 68: 508–512.

Freudenberg, K. (1968). The constitution and biosynthesis of lignin. In: Freudenberg, K., and Neish, A.C. (Eds.), *Constitution and biosynthesis of lignin*. Springer, Berlin, pp. 47–74.

Gottlieb, H.E., Kotlyar, V., and Nudelman, A. (1997). NMR chemical shifts of common laboratory solvents as trace impurities. J. Org. Chem. 62: 7512–7515.

Grabber, J.H., Hatfield, R.D., and Ralph, J. (2003). Apoplastic pH and monolignol addition rate effects on lignin formation and cell wall degradability in maize. J. Agric. Food Chem. 51: 4984–4989.

Harman-Ware, A.E., Happs, R.M., Davison, B.H., and Davis, M.F. (2017). The effect of coumaryl alcohol incorporation on the structure and composition of lignin dehydrogenation polymers. Biotechnol. Biofuels 10: 281.

Hilgers, R., Vincken, J.P., Gruppen, H., and Kabel, M.A. (2018). Laccase/mediator systems: their reactivity toward phenolic lignin structures. ACS Sustain. Chem. Eng. 6: 2037–2046.

Hofrichter, M., Vares, T., Kalsi, M., Galkin, S., Scheibner, K., Fritsche, W., and Hatakka, A. (1999). Production of manganese peroxidase and organic acids and mineralization of ^{14}C-labelled lignin (^{14}C-DHP) during solid-state fermentation of wheat straw with the white rot fungus *Nematoloma frowardii*. Appl. Environ. Microbiol. 65: 1864–1870.

Holmgren, A., Zhang, L., and Henriksson, G. (2008a). Monolignol dehydrogenative polymerization *in vitro* in the presence of dioxane and a methylated β-β′ dimer model compound. Holzforschung 62: 508–513.

Holmgren, A., Henriksson, G., and Zhang, L. (2008b). Effects of a biologically relevant antioxidant on the dehydrogenative polymerization of coniferyl alcohol. Biomacromolecules 9: 3378–3382.

Hwang, H., Moon, S.J., Won, K., Kim, Y.H., and Choi, J.W. (2015). Parameters affecting *in vitro* monolignol couplings during dehydrogenative polymerization in the presence of peroxidase and H_2O_2. J. Ind. Eng. Chem. 26: 390–395.

Ikeda, R., Sugihara, J., Uyama, H., and Kobayashi, S. (1998). Enzymatic oxidative polymerization of 4-hydroxybenzoic acid derivatives to poly(phenylene oxide)s. Holzforschung 47: 295–301.

Ikeda, T., Holtman, K., Kadla, J.F., Chang, H.M., and Jameel, H. (2002). Studies on the effect of ball milling on lignin structure using a modified DFRC method. J. Agric. Food Chem. 50: 129–135.

Jacquet, G., Pollet, B., Lapierre, C., Francesch, C., Rolando, C., and Faix, O. (1997). Thioacidolysis of enzymatic dehydrogenation polymers from *p*-hydroxyphenyl, guaiacyl, and syringyl precursors. Holzforschung 51: 349–354.

Johjima, T., Itoh, N., Kabuto, M., Tokimura, F., Nakagawa, T., Wariishi, H., and Tanaka, H. (1999). Direct interaction of lignin and lignin peroxidase from Phanerochaete chrysosporium. Proc. Natl. Acad. Sci. U.S.A. 96: 1989–1994.

Kilpeläinen, I., Sipilä, J., Brunow, G., Lundquist, K., and Ede, R.M. (1994). Application of two-dimensional NMR spectroscopy to wood lignin structure determination and identification of some minor structural units of hard- and softwood lignins. J. Agric. Food Chem. 42: 2790–2794.

Kim, H., Ralph, J., and Akiyama, T. (2008). Solution-state 2D NMR of ball-milled plant cell wall gels in DMSO-d_6. Bioenergy Res. 1: 56–66.

Kishimoto, T., Chiba, W., Saito, K., Fukushima, K., Uraki, Y., and Ubukata, M. (2010). Influence of syringyl to guaiacyl ratio on the structure of natural and synthetic lignins. J. Agric. Food Chem. 58: 895–901.

Lapierre, C., Pollet, B., Monties, B., and Rolando, C. (1991). Thioacidolysis of spruce lignin: GC-MS analysis of the main dimers recovered after raney nickel desulphuration. Holzforschung 45: 61–68.

Li, Q., Koda, K., Yoshinaga, A., Takabe, K., Shimomura, M., Hirai, Y., Tamai, Y., and Uraki, Y. (2015). Dehydrogenative polymerization of coniferyl alcohol in artificial polysaccharides matrices: effects of xylan on the polymerization. J. Agric. Food Chem. 63: 4613–4620.

Liitia, T.M., Maunu, S.L., Hortling, B., Toikka, M., and Kilpelainen, I. (2003). Analysis of technical lignins by two- and three-dimensional NMR spectroscopy. J. Agric. Food Chem. 51: 2136–2143.

Mechin, V., Baumberger, S., Pollet, B., and Lapierre, C. (2007). Peroxidase activity can dictate the *in vitro* lignin dehydrogenative polymer structure. Phytochemistry 68: 571–579.

Nakamura, R., Matsushita, Y., Umemoto, K., Usuki, A., and Fukushima, K. (2006). Enzymatic polymerization of coniferyl alcohol in the presence of cyclodextrins. Biomacromolecules 7: 1929–1934.

Pan, X.J. (2008). Role of functional groups in lignin inhibition of enzymatic hydrolysis of cellulose to glucose. J. Biobased Mater. Bioenergy 2: 25–32.

Pu, Y., Hu, F., Huang, F., and Ragauskas, A.J. (2015). Lignin structural alterations in thermochemical pretreatments with limited delignification. Bioenergy Res. 8: 992–1003.

Ragauskas, A.J., Beckham, G.T., Biddy, M.J., Chandra, R., Chen, F., Davis, M.F., Davison, B.H., Dixon, R.A., Gilna, P., Keller, M., et al. (2014). Lignin valorization: improving lignin processing in the biorefinery. Science 344: 709–719.

Ralph, J., Lundquist, K., Brunow, G., Lu, F., Kim, H., Schatz, P.F., Marita, J.M., Hatfield, R.D., Ralph, S.A., Christensen, J.H., et al. (2004). Lignins: natural polymers from oxidative coupling of 4-hydroxyphenylpropanoids. Phytochemistry Rev. 3: 29–60.

Rinaldi, R., Jastrzebski, R., Clough, M.T., Ralph, J., Kennema, M., Bruijnincx, P.C., and Weckhuysen, B.M. (2016). Paving the way for lignin valorisation: recent advances in bioengineering, biorefining and catalysis. Angew. Chem. Int. Ed. 55: 8164–8215.

Roland, C., Monties, B., and Lapierre, C. (1992). Thioacidolysis. In: Lin, S.Y., and Dence, C.W. (Eds.), *Methods in lignin chemistry*. Springer, Berlin, pp. 334–349.

Saake, B., Argyropoulos, D.S., Beinhoff, O., and Faix, O. (1996). A comparison of lignin polymer models (DHPs) and lignins by ^{31}P NMR sepctroscopy. Phytochemistry 43: 499–507.

Sarkanen, K.V. (1971). Precursors and their polymerization. In: Sarkanen, K.V., and Ludwig, C.H. (Eds.), *Lignins- Occurrence, formation, structure and reactions*. Wiley-Interscience, New York, pp. 95–163.

Sturgeon, M.R., Kim, S., Lawrence, K., Paton, R.S., Chmely, S.C., Nimlos, M., Foust, T.D., and Beckham, G.T. (2014). A mechanistic investigation of acid-catalyzed cleavage of aryl-ether linkages: implications for lignin depolymerization in acidic environments. ACS Sustain. Chem. Eng. 2: 472–485.

Tanahashi, M. and Higuchi, T. (1990). Effect of the hydrophobic regions of hemicellulose on dehydrogenative polymerization of sinapyl alcohol. Mokuzai Gakkaishi 36: 424–428.

Terashima, N., Atalla, R.H., Ralph, S.A., Landucci, L.L., Lapierre, C., and Monties, B. (1995). New preparations of lignin polymer models under conditions that approximate cell wall lignification. I. Synthesis of novel lignin polymer models and their structural characterization by ^{13}C NMR. Holzforschung 49: 521–527.

Terashima, N., Atalla, R.H., Ralph, S.A., Landucci, L.L., Lapierre, C., and Monties, B. (1996). New preparations of lignin polymer models under conditions that approximate cell wall lignification. II. Structural characterization of the models by thioacidolysis. Holzforschung 50: 9–14.

Terashima, N., Akiyama, T., Ralph, S., Evtuguin, D., Neto, C.P., Parkås, J., Paulsson, M., Westermark, U., and Ralph, J. (2009). 2D-NMR (HSQC) difference spectra between specifically ^{13}C-enriched and unenriched protolignin of *Ginkgo biloba* obtained in the solution state of whole cell wall material. Holzforschung 63: 379–384.

Tijssen, P. (1985). Properties and preparation of enzymes used in enzyme-immunoassays. In: Burdon, R.H., and van Knippenberg, P.H. (Eds.), *Practice and theory of enzyme immunoassays*. Elsevier, New-York, pp. 173–220.

Tobimatsu, Y., Takano, T., Kamitakahara, H., and Nakatsubo, F. (2006). Studies on the dehydrogenative polymerizations of monolignol beta-glycosides. Part 2: horseradish peroxidase catalyzed dehydrogenative polymerization of isoconiferin. Holzforschung 60: 513–518.

Tokunaga, Y., Nagata, T., Suetomi, T., Oshiro, S., Kondo, K., Katahira, M., and Watanabe, T. (2019). NMR analysis on molecular interaction of lignin with amino acid residues of carbohydrate-binding module from *Trichoderma reesei* Cel7A. Sci. Rep. 9: 1977.

Tokunaga, Y., Nagata, T., Kondo, K., Katahira, M., and Watanabe, T. (2021). Complete NMR assignment and analysis of molecular structural changes of β–*O*–4 lignin oligomer model compounds in organic media with different water content. Holzforschung 75: 379–389.

van Parijs, F.R.D., Morreel, K., Ralph, J., Boerjan, W., and Merks, R.M. (2010). Modeling lignin polymerization. I. Simulation model of dehydrogenation polymers. Plant Physiol. 153: 1332–1344.

Yue, F., Lu, F., Sun, R.C., and Ralph, J. (2012). Syntheses of lignin-derived thioacidolysis monomers and their uses as quantitation standards. J. Agric. Food Chem. 60: 922–928.

Zeng, J., Helms, G.L., Gao, X., and Chen, S. (2013). Quantification of wheat straw lignin structure by comprehensive NMR analysis. J. Agric. Food Chem. 61: 10848–10857.

Zhang, L., Gellerstedt, G., Ralph, J., and Lu, F. (2006). NMR studies on the occurrence of spirodienone structures in lignins. J. Wood Chem. Technol. 26: 65–79.